geosciences

MDPI

Article

Geochemical Features of the Weathered Materials Developed on Gabbro in a Semi-Arid Zone, Northern Cameroon

Désiré Tsozué [1,*] and Paul-Désiré Ndjigui [2]

[1] Department of Earth Sciences, University of Maroua, P.O. Box 814, Maroua, Cameroon
[2] Department of Earth Sciences, University of Yaoundé 1, P.O. Box 812, Yaoundé, Cameroon; lndjigui@yahoo.fr
* Correspondence: tsozudsir@yahoo.fr or desire.tsozue@fs.univ-maroua.cm; Tel.: +237-675-121-489

Academic Editors: Carlos Alves and Jesús Martínez Frías
Received: 22 January 2017; Accepted: 15 March 2017; Published: 27 March 2017

Abstract: Investigation on the mobilization and the redistribution of major, trace and rare-earth elements (REE) was performed along a soil profile developed on gabbro in the semi-arid zone (Northern Cameroon), using mineralogical and geochemical analyses. The gabbro has high contents in Ba, Cr, V, Sr, Ni, Zn, Zr, Cu, Co and Sc. The total REE content is 49 mg/kg with strong light rare-earth elements (LREE) abundance. The Ce/Ce* and Eu/Eu* ratios are very close to 1 (0.98 and 1.02 respectively) and the $(La/Yb)_N$ ratio is very low (1.48). The weathering of the bedrock leads to the differentiation of coarse saprolite, fine saprolite, loamy clayey horizon and humiferous horizon. Among trace elements, Cr and Zr concentrations range between 50 and 150 mg/kg; Ga, Y, Co, Cu, Ni and Sc concentrations vary between 50 and 150 mg/kg while those of Cs, Hf, Nb, Rb, Sn, Ta, Th, U and Pb are below 5 mg/kg. The total REE contents vary from 62.52 to 78.81 mg/kg, with strong LREE abundance. The values of the $(La/Yb)_N$ ratio (~1.04–1.59) is low and indicate the low REE fractionation. Negative Ce anomaly (Ce/Ce* ~ 0.86) and positive Eu anomalies (Eu/Eu* ~ 1.22) are observed respectively in the middle part and the whole soil profile. Mass balance calculation reveals the leaching of Ca, Mg, K, Ba, Cr, Rb, Co, Cu, Ni, Al, Cs, Sr, U and V, and accumulation of Si, Fe, Ti, Mn, Na, P, Ga, Hf, Nb, Sn, Ta, Y, Zr, Sc, Zn and REE during the weathering.

Keywords: gabbro; weathered materials; geochemistry; mass balance; semi-arid zone; Northern Cameroon

1. Introduction

Many works have been done on the behaviour of chemical elements in the weathering materials developed under various parent rocks [1–4]. In the Central African region, the studies are concentrated mainly in the humid tropical zone, characterised by the formation of large thick weathering mantles. They globally present various complex soil profiles due to climate fluctuations in the past, which generates controversial interpretations [5,6]. This complexity varies depending on whether one is on ultramafic rocks or not. The behaviour of the element varies according to the nature of the bedrock. It also depends on the minerals present and the prevailing mechanisms of weathering. Several authors [2,6] have noticed the presence of cerium anomalies in the saprolite zone. Bayiga et al. [7] reported a relative accumulation of Si, Al, Fe and K, an accumulation of Ru, Ba, Zr, Hf, V, Sn and Pb, and a depletion of Sr, Zn, Co, Y and most rare-earth elements (REE) in soil profile developed on amphibolites. Those works were essentially concentrated in the humid tropical zone, whereas the climate varies according to latitude in the tropics. This variation is well represented in Cameroon. Contrary to Southern Cameroon, the northern region, where a Sudano-Sahelian climate prevails, remains poorly known, and studies on the element behaviour alongside the soil profile are scarce.

Nguetnkam et al. [8] carried out mineralogical and geochemical investigations in this area, but did not specify the location and type of rock on which their study was done. The aim of the present study is to document and explain the distribution of major, trace and REE along a soil profile developed on gabbro at the eastern extremity of the Mandara Mountains, in the semi-arid zone.

2. Materials and Methods

2.1. Study Site

The study area is located in Maroua, in Northern Cameroon. It extends globally between 10°35′00″ N and 10°40′30″ N and between 14°16′04″ E and 14°21′34″ E (Figure 1). The climate is Sudano-Sahelian [9]. The mean annual rainfall is 757.2 mm. The mean annual air temperature is about 28.53 °C. The relief is mountainous, characterised globally by gentle to steep slopes. The vegetation is mostly composed of grasses [10]. The study area is an extension of the Poli series [11]. It is formed at the base by a lower to middle Precambrian basement (500 to 600 Ma), mesozonal to catazonal, composed mainly of gneisses and migmatites. This basement is intruded on by many rock types, of which gabbros are the dominant formations [12,13].

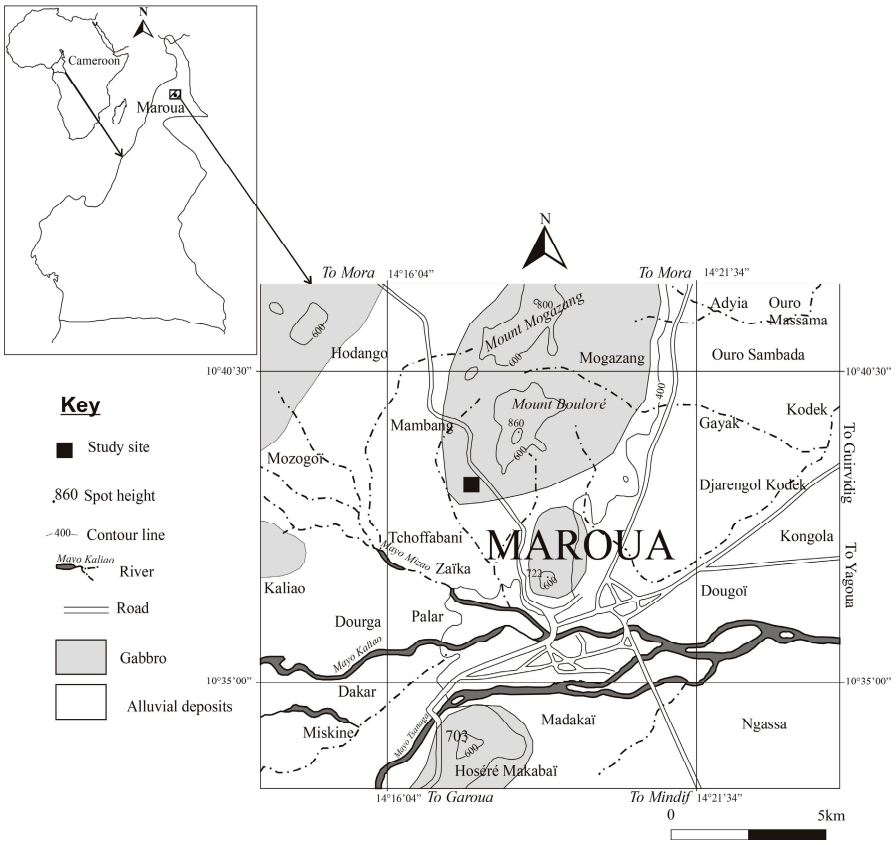

Figure 1. Location and geological map of the study site.

2.2. Field and Laboratory Methods

Fieldwork consisted firstly of many exploration test auger boreholes made on several expeditions in order to choose the interfluve on which the study should been done. On the chosen interfluve, one pit, located at the middle slope where the soil profile is deep enough for studying the redistribution of major, trace and REE, was dug manually.

Field descriptions allow us to note that the studied weathered materials are composed of four main horizons, from bottom to top, as follows (Figure 2):

- Coarse saprolite (200–75 cm): yellowish (10YR 7/8) horizon. It is compact, massive, and characterised by many fissures surrounding compact undifferentiated blocks; the original structure of the bedrock is preserved; the mean bulk density and pH are 2.35 g/cm^3 and 7.5 at the bottom (Ma2) and 2.23 g/cm^3 and 7.6 at the upper part (Ma3) of the horizon; in the upper part, the colour becomes reddish yellow (7.5YR 7/8);
- Fine saprolite (75–30 cm): reddish yellow (7.5YR 6/8) horizon, characterised by a loamy texture and a massive structure. There are many fissures surrounding small grey compact blocks, globally embedded in a loose matrix; the structure of the bedrock was preserved in grey compact blocks; the bulk density is 1.84 g/cm^3 and the pH is 7.8 (Ma4);
- Loose loamy clayey texture horizon (30–7 cm); reddish yellow (5YR 6/8) horizon; it had a weakly blocky to massive structure, a high matrix porosity and many rootlets; its mean bulk density is 1.30 g/cm^3 and the pH is 6.7 (Ma5);
- Humiferous horizon (7–0 cm); yellowish red (5YR 5/8) horizon, characterised by a loamy clayey texture and a weakly expressed lumpy structure, high matrix porosity and the presence of many rootlets; its mean bulk density is 1.10 g/cm^3 and the pH is 6.5 (Ma6).

After pit description, weathered materials and fresh rock samples were thereafter collected, air-dried and crushed into a fine powder prior to analyses.

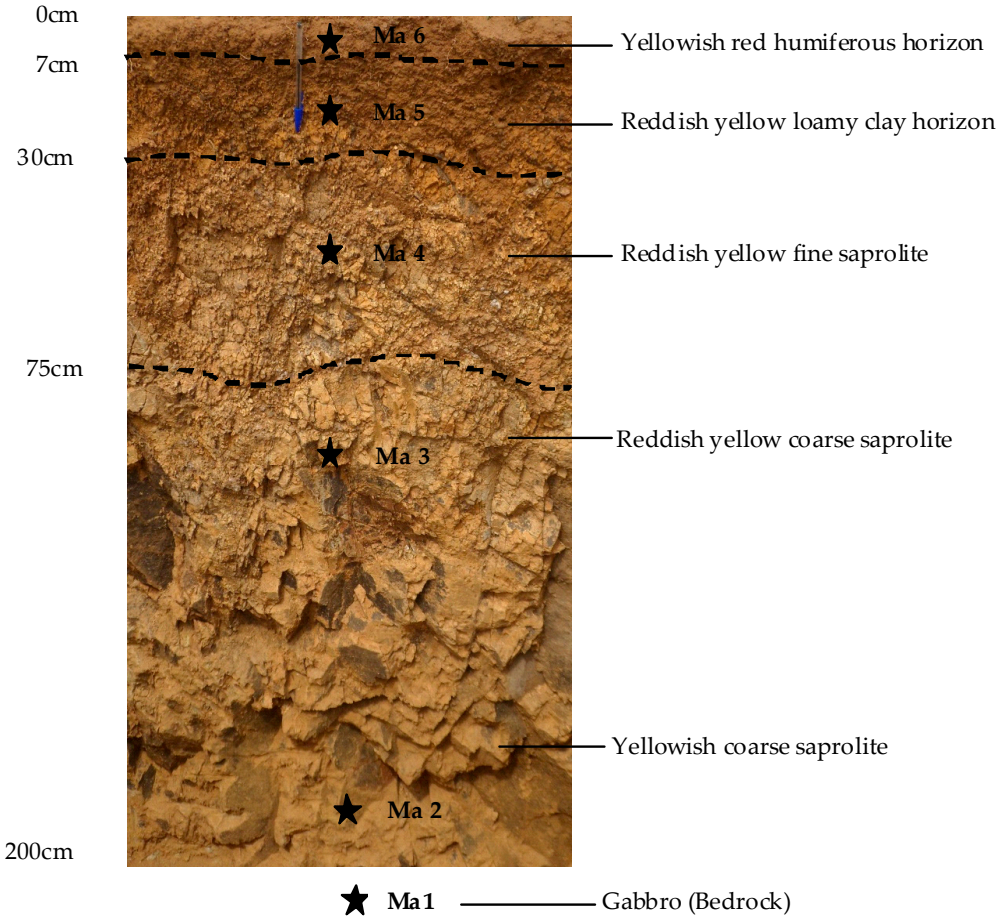

Figure 2. Morphological characteristics of the soil profile studied in the Maroua region (Cameroon). (Stars are sampling points; discontinuous lines are boundaries between horizons.)

In the laboratory, soil pH was measured potentiometrically in a 1:2.5 soil:solution ratio [14]. Bulk density was determined by the clod method [15]. Mineral assemblage was performed using polarizing

microscope (Jeulin, Evreux, France) on thin sections from representative gabbro samples. Soil mineralogy was determined by X-ray diffraction (XRD) and Fourier transform infrared spectroscopy (FTIR) on total soil powder. Clay fraction was not separated. X-ray diffraction patterns were recorded at room temperature using a classical powder diffractometer (X'pert Pro PW3710, Philips, Amsterdam, The Netherlands) instrument equipped with Ni-filtered and Cu anode (quartz monochromator, K-α1 wavelength = 1.5405600Å) operating at 45 kV and 40 mA. This Philips PW3710 instrument operates in continuous scan mode and in step scan mode range from 2° to 70°, with 2θ step of 0.02° and counting time of 0.50 s per step. Minerals were identified using XRD coupled with standard saturation (K), solvation (ethylene glycol), and heat (550 °C) treatments [16].

Diffuse reflectance infrared spectra were recorded between 4000 and 400 cm^{-1}, using a FTIR Perkin Elmer 2000 spectrometer (Perkin Elmer, Waltam, MA, USA) equipped with deuterated triglycine sulfate (DTGS) detector. Air-dried samples were analysed at room temperature using Diamond Attenuated Total Reflectance (ATR) accessories (Perkin Elmer). The spectrum resolution was 4 cm^{-1} and the accumulation time was 5 min.

For geochemical analysis, all samples were pulverized to obtain a homogeneous sample and 50–60 g were used for the analyses. Chemical analysis was done using the pulp at ALS Minerals Global Group, Vancouver, Canada. The details of different methods used are available at www.alsglobal.com. Lab codes are ME-MS81D (ME-MS81 plus whole rock), ME-4ACD81 (base metals by four-acid digestion). Whole-sample analyses for major elements were done by Inductively Coupled Plasma-Atomic Emission (ICP-AES) and trace elements were carried out by Inductively Coupled Plasma Mass Spectrometry (ICP-MS) from pulps. For this purpose, 0.2 g of sample powder is added to 1.5 g lithium metaborate ($LiBO_2$), mixed well and fused in a furnace at 1000 °C. The resulting melt is then cooled and dissolved in 100 mm^3 of 5% HNO_3 acid solution. The REE contents were determined by ICP-MS from pulps after 0.25 g sample powder was dissolved with four acid digestions. Analytical uncertainties varied from 0.1% to 0.04% for major elements; 0.1% to 0.5% for trace elements; and 0.01 to 0.5 mg/kg for rare earth elements. The remaining trace elements were analysed by ICP-MS after 0.5 g split of sample pulp was digested in aqua regia. Loss on ignition (LOI) was determined by weight difference after ignition at 1000 °C. Various standards were used and data quality assurance was verified by running these standards between samples as unknowns. Analytical uncertainties were currently better than 1% for major elements and 5%–6% for trace elements concentrations. Analysis precision for rare earth elements was estimated at 5% for concentrations >10 mg/kg and 10% when lower.

The behaviour of chemical elements throughout the weathering mantle was assessed by calculating elements' mass balance during weathering. These mass balances were done according to a calculated 'mass balance method' [17,18] by considering Th as an invariant element [6]. Thorium is often located in the same accessory minerals as REEs in plutonic and metamorphic rocks, thus enabling it to be used as a relative internal standard for these elements. Mass balance is based on the residual enrichment in closed systems and supergene enrichment in open systems, which has previously required the determination of horizon deformation rates. This method enables us to estimate the quantity of each element that is depleted or accumulated [19]. The horizon deformation rate (ε) and element mobilization rate (τ) in each horizon are calculated according to the following formulae:

$$\varepsilon_a = \frac{C_{i,p}.d_p}{C_{i,a}.d_a} - 1$$

$$\tau_{j,a} = \frac{d_a}{d_p}\frac{C_{j,a}}{C_{j,p}}(\varepsilon_a + 1) - 1$$

In these formulae, $C_{i,p}$ and $C_{i,a}$ are the concentrations of an invariant element i (here: Th) in the parent rock p and the horizon a, respectively; $C_{j,p}$ and $C_{j,a}$ are concentrations of any common element j, respectively, in the parent rock p and the horizon a; and d_p and d_a are the bulk density of the parent rock p and the horizon a , respectively [3,20].

3. Results

3.1. Petrology of Gabbro

The bedrock is a gabbro according to the chemical classification of Middlemost [21]. It outcropped as small massifs in the study area and was the most represented formation. Macroscopically, it is dark, massive, and characterised by white slight linings and the absence of any observable mineral. Under a polarizing microscope, the rock was mainly composed of plagioclase and green amphibole, and accessory minerals such as biotite, calcite and alkaline feldspar. Its mean bulk density was 2.90 g/cm^3 (Ma1). From a geochemical point of view, among the major elements, the SiO_2 contents were high (48.90 wt %). The other significant concentrations were those of Al_2O_3 (16.95 wt %), Fe_2O_3 (10.55 wt %), CaO (9.55 wt %), MgO (6.87 wt %) and Na_2O (2.50 wt %) (Table 1). Gabbro has high contents of Ba, Cr, V, Sr, Ni, Zn, Zr, Cu, Co and Sc. Other elements, like Ga, Y and Rb, present low contents (Table 1). The total REE content is 49 mg/kg with low enrichment in light REE relative to heavy REE (LREE/HREE = 2.25). LREE were largely dominated by Ce (12.90 mg/kg) and Nd (9.90 mg/kg) (Table 1). On the other hand, HREE were mainly represented by Dy (4.10 mg/kg), Gd (3.49 mg/kg), Er (2.50 mg/kg) and Yb (2.21 mg/kg) (Table 1). The REE normalised to chondrite according to McDonough and Sun [22], and, as shown in Figure 3, revealed moderate LREE enrichment and slight HREE enrichment. The Ce/Ce* and Eu/Eu* ratio values are close to 1 (Table 1). The $(La/Yb)_N$ ratio is very low (1.48).

Table 1. Major element (wt %), trace element (mg/kg) and rare-earth elements (REE) (mg/kg) contents obtained by geochemical analysis for the soil profile samples in the Maroua region (Cameroon).

Elements	dl	Ma1	Ma2	Ma3	Ma4	Ma5	Ma6
SiO_2	0.01	48.90	53.90	53.10	52.10	51.60	50.80
Al_2O_3	0.01	16.95	15.00	14.70	15.55	16.25	15.90
Fe_2O_3	0.01	10.55	10.75	10.90	11.20	11.80	11.85
CaO	0.01	9.55	1.02	4.22	3.23	3.02	5.12
MgO	0.01	6.87	2.06	1.76	1.78	1.68	1.76
Na_2O	0.01	2.50	4.11	4.33	4.76	3.55	3.02
K_2O	0.01	1.17	0.46	0.27	0.31	0.24	0.30
TiO_2	0.01	1.15	1.06	1.14	1.20	1.23	1.20
MnO	0.01	0.17	0.22	0.23	0.24	0.31	0.27
P_2O_5	0.01	0.20	0.22	0.28	0.21	0.08	0.10
LOI	0.01	3.38	9.05	8.88	10.10	11.50	10.30
Ba	0.50	771.00	400.00	300.00	393.00	375.00	322.00
Cr	10.00	310.00	50.00	50.00	40.00	50.00	90.00
Cs	0.01	0.08	0.03	0.07	0.06	0.06	0.12
Ga	0.10	18.30	21.00	19.80	20.00	22.20	23.20
Hf	0.20	2.10	2.60	2.20	2.21	2.20	3.00
Nb	0.20	2.20	2.60	2.20	2.30	2.50	3.00
Rb	0.20	13.40	3.50	2.40	2.40	2.20	4.00
Sn	1.00	1.00	1.00	1.00	1.00	1.00	1.00
Sr	0.10	291.00	261.00	304.00	218.00	221.00	317.00
Ta	0.10	0.10	0.20	0.10	0.10	0.20	0.20
Th	0.05	0.33	0.31	0.22	0.24	0.37	1.09
Tl	0.05	<dl	<dl	<dl	<dl	<dl	<dl
U	0.05	0.15	0.13	0.10	0.11	0.14	0.35
V	5.00	292.00	271.00	272.00	242.00	280.00	308.00
W	1.00	<dl	<dl	<dl	<dl	<dl	<dl
Y	0.50	22.10	28.70	27.50	27.70	27.00	29.20
Zr	2.00	68.00	87.00	73.00	70.00	76.00	105.00
Ag	0.50	<dl	<dl	<dl	<dl	<dl	<dl
As	5.00	<dl	<dl	<dl	<dl	<dl	<dl

Table 1. *Cont.*

Elements	dl	Ma1	Ma2	Ma3	Ma4	Ma5	Ma6
Cd	0.50	<dl	<dl	<dl	<dl	<dl	<dl
Co	1.00	39.00	24.00	26.00	24.00	30.00	26.00
Cu	1.00	64.00	5.00	2.00	1.00	10.00	30.00
Li	10.00	10.00	<dl	<dl	<dl	<dl	<dl
Mo	1.00	<dl	<dl	<dl	<dl	<dl	<dl
Ni	1.00	97.00	12.00	12.00	12.00	13.00	12.00
Pb	2.00	<dl	4.00	3.00	<dl	<dl	3.00
Sc	1.00	28.00	31.00	33.00	34.00	36.00	34.00
Zn	2.00	81.00	163.00	155.00	155.00	159.00	131.00
La	0.50	4.80	6.90	6.10	7.10	7.30	9.90
Ce	0.50	12.90	17.70	15.10	15.70	18.50	23.30
Pr	0.03	2.13	2.79	2.52	2.88	2.88	3.53
Nd	0.10	9.90	13.00	12.10	14.00	13.50	15.8
Sm	0.03	3.04	4.02	3.84	4.20	4.01	4.62
Eu	0.03	1.16	1.63	1.67	1.81	1.78	2.04
Gd	0.05	3.99	5.16	4.94	5.44	5.19	5.48
Tb	0.01	0.67	0.87	0.82	0.89	0.83	0.88
Dy	0.05	4.10	2.22	4.96	5.24	4.97	5.23
Ho	0.01	0.88	1.14	1.05	1.13	1.07	1.14
Er	0.03	2.50	3.17	3.00	2.99	2.92	3.10
Tm	0.01	0.36	0.47	0.43	0.44	0.43	0.45
Yb	0.03	2.21	2.97	2.70	2.68	2.64	2.87
Lu	0.01	0.36	0.48	0.42	0.39	0.41	0.47
ΣREE	-	49.00	62.52	59.65	64.89	66.43	78.81
LREE	-	33.93	46.04	41.33	45.69	47.97	59.19
HREE	-	15.07	16.48	18.32	19.20	18.46	19.62
LREE/HREE	-	2.25	2.80	2.26	2.38	2.60	3.02
$(La/Yb)_N$ (1)	-	1.48	-	-	-	-	-
$(La/Yb)_N$ (2)	-	-	1.06	1.04	1.22	1.27	1.59
Ce/Ce* (1)	-	0.98	-	-	-	-	-
Ce/Ce* (2)	-	-	1.00	0.95	0.86	1.00	0.98
Eu/Eu* (1)	-	1.02	-	-	-	-	-
Eu/Eu* (2)	-	-	1.07	1.15	1.14	1.17	1.22

Ma: Sampling points (sample descriptions are illustrated in Figure 2); dl: detection limit. $(La/Yb)_N$ (1): $(La_{gabbro}/La_{chondrite})/(Yb_{gabbro}/Yb_{chondrite})$; $(La/Yb)_N$ (2): $(La_{soil\ sample}/La_{gabbro})/(Yb_{soil\ sample}/Yb_{gabbro})$; Ce/Ce* (1): $(Ce_{gabbro}/Ce_{chondrite})/(La_{gabbro}/La_{chondrite})^{1/2}(Pr_{gabbro}/Pr_{chondrite})^{1/2}$; Ce/Ce* (2): $(Ce_{soil\ sample}/Ce_{gabbro})/(La_{soil\ sample}/La_{gabbro})^{1/2}(Pr_{soil\ sample}/Pr_{gabbro})^{1/20}$; Eu/Eu* (1): $(Eu_{gabbro}/Eu_{chondrite})/(Sm_{gabbro}/Sm_{chondrite})^{1/2}(Gd_{gabbro}/Gd_{chondrite})^{1/2}$; Eu/Eu* (2): $(Eu_{soil\ sample}/Eu_{gabbro})/(Sm_{soil\ sample}/Sm_{gabbro})^{1/2}(Gd_{soil\ sample}/Gd_{gabbro})^{1/2}$.

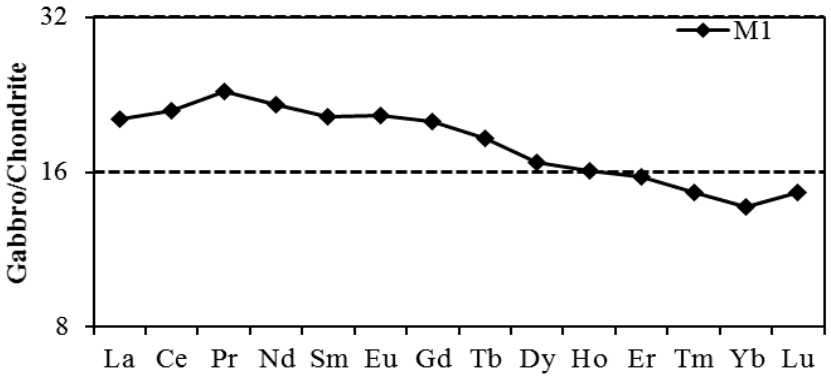

Figure 3. Chondrite-normalized (McDonough and Sun [20]) rare-earth element pattern for gabbro.

3.2. Petrology of Weathering Materials

3.2.1. Mineralogical Characterisation

In the X-ray spectra, except for the humiferous surface horizon (Ma6), all horizons presented peaks at 15.48 Å in the air-dried sample, which shifted to about 10 Å after heating at 550 °C (Figure 4). These peaks shifted to 17.64 Å after treatment with ethylene glycol. In the dark humiferous horizon, only the 10 Å peak was present in the spectrum of the air-dried sample. It remained at 10 Å after heating at 550 °C, but shifted immediately to 17.64 Å after treatment with ethylene glycol (Figure 4). This indicates the presence of montmorillonite. Its presence was confirmed by the 4.6 Å peak. Sepiolite, a Mg fibrous phyllosilicate 2:1 close to trioctahedral phyllosilicate is present. It is identified by its peaks at 4.29 and 2.56 Å. Kaolinite is recognized by its peak at 7.1 Å, which, except in the humiferous surface horizon, is present in the spectra of different air-dried samples, but disappeared completely after heating at 550 °C (Figure 4). Its presence is confirmed by the peak at 3.57 Å, which appeared in all spectra regardless of the treatment. The peak at 3.89 Å might be attributed to calcite because this mineral is frequently observed in the studied area [23], although the peak at 3.03 Å is not visible. As for iron oxides, they are represented by goethite (4.1 and 2.45 Å) and its polymorph lepidocrocite (6.5 and 2.97 Å), which fitted in with the yellowish soil colour observed in the field. As for aluminium oxides, only gibbsite is present, identified by its peaks at 4.8 and 2.39 Å. Beyond these secondary minerals, feldspar is noted, and the main peak highly developed in all spectra at 3.24 Å showed that this feldspar mineral is microcline (Figure 4). Quartz is identified by peaks at 4.29, 3.37, 2.12 and 1.82 Å.

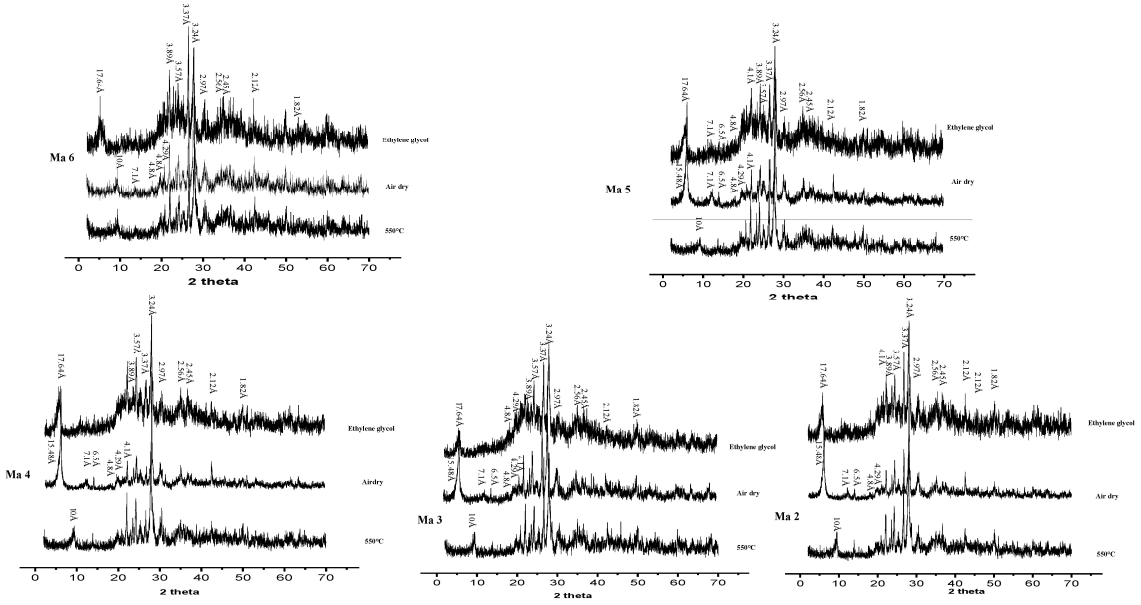

Figure 4. X-ray diffractograms for the studied soils from the Maroua region (Cameroon).

In FTIR spectra of the different analysed soil samples, the mineralogical composition reflected that obtained in XRD. Montmorillonite is identified by peaks at 1633 and 1634 cm^{-1} (Figure 5). Sepiolite is identified by peaks at 784 and 523 cm^{-1}. Kaolinite is characterised by peaks at 3694, 3617, 3616, 910, 759, 758, 760 and 757 cm^{-1}. Peaks at 3692, 3693 and 3694 cm^{-1} are also attributed to brucite $Mg_3(OH)_6$ since they were closed to 3696 cm^{-1}, which is the peak suggested by Mella and Mermut [24] to brucite (Figure 5). This mineral often occurs in association with calcite, already detected in XRD but not identified here. Gibbsite is detectable thanks to peaks at 3616, 3617, 3375, 3383, 990 and 571 cm^{-1} and shoulders noted at 985 and 1070 cm^{-1} (Figure 5). Goethite is observable by peaks at 680, 677, 675, 646, 410, 405 cm^{-1} and characteristic bands of 880–900 cm^{-1}. Lepidocrocite, still present as in X-ray patterns, is recognized by its peak at 743 cm^{-1} (Figure 5). Also, weak absorption at 3616 and

3617 cm^{-1}, consistent with the more limited development of its face (010) and its smaller specific surface area, and 3564–3572 cm^{-1} was tentatively assigned to its (100) face [25]. Quartz is identified in different spectra at 783, 784, 785, 494, 495, 498 and 499 cm^{-1} (Figure 5).

The studied soils were composed of montmorillonite, sepiolite, brucite, kaolinite, gibbsite, goethite, lepidocrocite, feldspar, calcite and quartz.

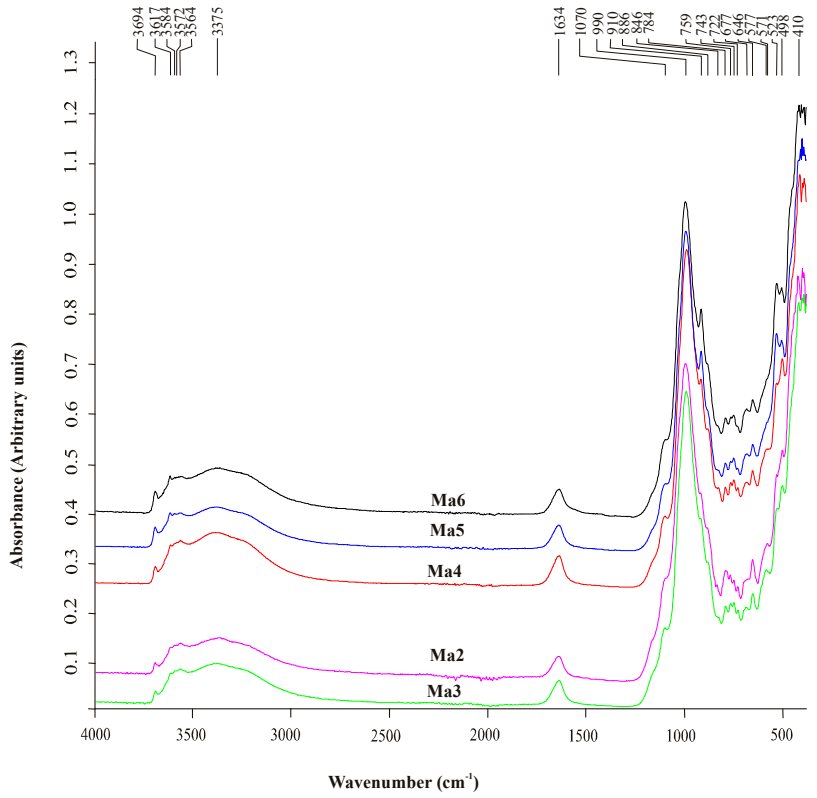

Figure 5. Infrared spectra of the studied soils from the Maroua region (Cameroon).

3.2.2. Geochemical Characteristics

Major elements

Apart from K_2O, MnO and P_2O_5 whose contents are less than 0.5 wt %, all the other major elements are present in higher amounts (Table 1). The concentration of SiO_2 is the highest among oxides. Its contents decrease slightly and gradually from the bottom to the upper part of the profile, varying from 53.90 to 50.80 wt %. Other major element contents are at least three times lower than those of SiO_2. Al_2O_3 contents varied from 14.70 to 16.25 wt %. The high value was recorded in the upper part of the profile. Fe_2O_3 contents, contrary to those of SiO_2, increased from the bottom to the top of the profile (Table 1). CaO contents strongly increase from the base to the top of the coarse saprolite, decrease from this zone to the reddish yellow loamy clayey horizon, and increase at last to the humiferous surface horizon. MgO contents vary slightly along the profile (Table 1). Na_2O presents different behaviour. It increases from the bottom to the middle part of the weathered profile and decrease thereafter to the humiferous surface horizon. TiO_2 contents varied little along the profile, increasing slightly from the bottom to the upper part of the profile (Table 1).

Trace elements

Five groups of trace elements were distinguished on the basis of their concentration and behaviour along the weathering profile:

- Elements with high concentrations in soil sample upper than 150 mg/kg are Ba, Sr, V, and Zn. From the bottom of the profile, Zn concentration, which is the lowest in this group, progressively decreases towards the humiferous horizon (Figure 6a). Sr and V show similar behaviour except in the saprolite zone, where V decreases while Sr increases (Figure 6a). Ba concentrations are the highest except in the middle part of the weathering profile, where they are similar to those of Sr. Globally, barium behaviour is opposite to that of Sr and V (Figure 6a);
- Elements of concentration between 50 and 150 mg/kg are Cr and Zr (Table 1). They show similar behaviour, but with high Zr concentrations (Figure 6b). This behaviour is close to that of V (Figure 6a,b);
- Elements whose contents varied between 5 and 50 mg/kg are Ga, Y, Co, Cu, Ni and Sc (Table 1). Sc concentrations are the highest (Table 1 and Figure 6c). Its behaviour is opposite to that of Y, Ni and Cu (Figure 6c). Cu exhibits lowest concentrations in the lower part of the weathering profile (Table 1 and Figure 6c). Co displays a zigzag signature (Figure 6c);
- Elements of low concentrations below 5 mg/kg are Cs, Hf, Nb, Rb, Sn, Ta, Th, U and Pb (Table 1). Among them Cs, Sn, Ta and U showed a similar trend and their concentrations vary slightly along the weathering profile (Figure 6d). Thorium, Hf and Nb concentrations decrease slightly from the base towards the middle part of the profile and increase progressively towards the humiferous surface (Figure 6d). Their behaviour was close to that of Zr and Cr (Figure 6d,b). Pb and Rb show a zigzag trend, as do Co and Ni (Figure 6d,c);
- Elements of concentrations below the detection limit, not detected in the studied soils, include Tl, Mo, W, Ag, As, Cd and Li (Table 1).

Rare-earth elements

The total REE contents vary between 41 and 78.81 mg/kg. Among LREE, Ce and Nd showed the highest concentrations. Among HREE, Gd and Dy have the highest concentrations (Table 1). LREE/HREE ratios are between 2.26 and 3.02. The $(La/Yb)_N$ ratios are higher than 1, ranging between 1.04 and 1.59 (Table 1). The highest value is recorded in the humiferous surface horizon, while the lowest one is noted in the middle part of the profile (Table 1). $(La/Yb)_N$ globally shows fractionation between LREE and HREE. Parent rock-normalized patterns revealed a similar behaviour of REE, except at the bottom and in the upper humiferous surface horizon (Figure 7). The Ce/Ce* ratios range between 0.86 and 1, and a slightly negative Ce anomaly is noticed in the middle part of the soil profile (Figure 7 and Table 1). Slight, positive Eu anomalies occur (Eu/Eu* = 1.07–1.22) (Figure 7 and Table 1).

Relative element mobility

The mass balance assessment approach, according to Ndjigui et al. [2], enables us to understand the mobility of elements in weathered materials. This was done by the estimating of losses and gains of matter expressed either in percent or kg/m^3 of the weathered parent material and are shown in Table 2. Relative mobility of elements along the soil profile showed three categories of elements: (i) elements depleted along the profile Ca, Mg, K, Ba, Cr, Rb, Co, Cu, and Ni (Table 2); (ii) elements depleted at the bottom and the top of the profile (Al, Ti, Cs, Sr, U and V) and (iii) elements depleted only in the upper part of the profile (Si, Fe, Mn, Na, P, Ga, Hf, Nb, Sn, Ta, Y, Zr, Sc, Zn, and REE).

The five elements Al, Cs, Sr, U and V present a negative mean mobilization rate varying from −5.95 to −22.68%, which implies that they were leached out of the profile. Ti, although depleted at the bottom and in the upper part of the profile, was accumulated in the soil profile, with a mean mobilization rate of 3.54% (Table 2).

Elements depleted in the upper part of the profile, which are Si, Fe, Mn, Na, P, Ga, Hf, Nb, Sn, Ta, Y, Zr, Sc, Zn, and REE, present a positive mean mobilization rate and were therefore enriched in the profile (Table 2). Among major and trace elements, Na and Zn are the most accumulated elements with a positive mean mobilization rate of 72% and 97.68%, respectively (Table 2). REE were depleted in the humiferous surface horizon except for Dy depleted at the base of the profile. Globally, the soils

are more enriched in LREE than in HREE. The mean mobilization rate of LREE varies from 34.42% to 54.12%, while that of HREE varies from 12.37% to 33.74% (Table 2).

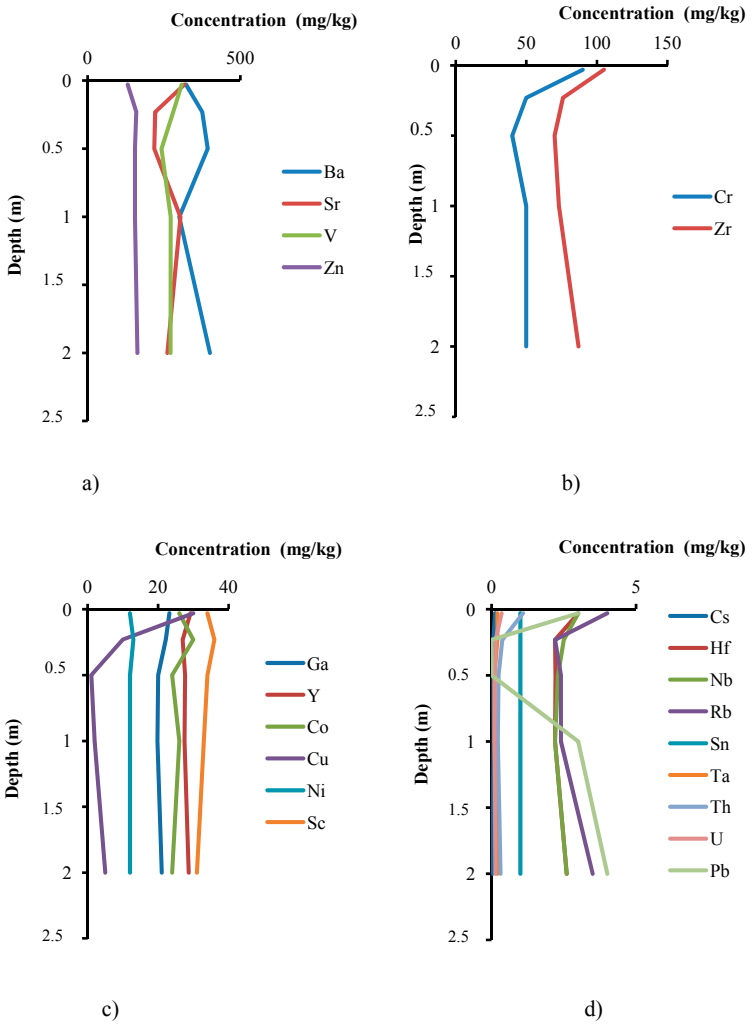

Figure 6. Evolution of trace elements with depth.

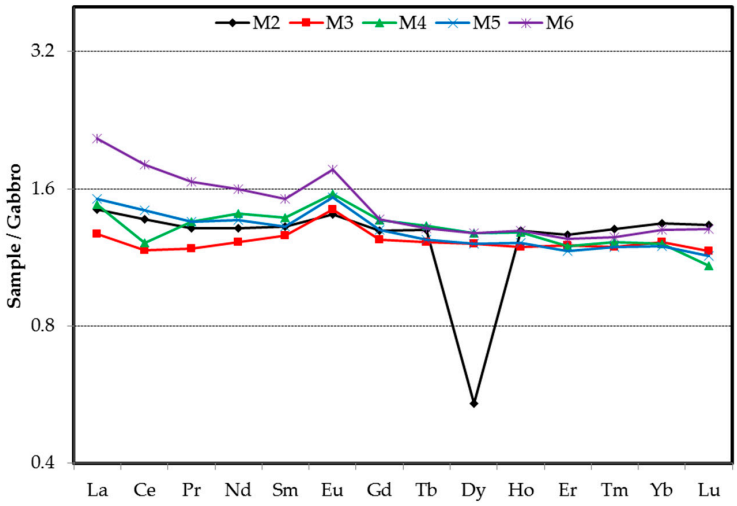

Figure 7. Gabbro-normalized rare-earth element patterns of the profile samples.

4. Discussion

4.1. Geochemistry of Gabbro

The chemical composition of the gabbro suggested an origin involving partial melting of mafic crustal material. The composition of this rock plotted in calc-alkaline field on an AFM diagram (A = Na_2O + K_2O, F = FeO + Fe_2O_3, M = MgO). Similar results were reported by Toteu et al. [26]. Al_2O_3/(Na_2O + K_2O) = 4.62 > 1 and Al_2O_3/((Na_2O + K_2O + CaO) = 1.28 are plotted as value of peraluminous rock type in conformity to S-type [27]. The low concentration of incompatible elements (e.g., La, Ba, Nb, and Th) ruled out the possibility that these rocks were produced by melting of the enriched lithospheric mantle [28], especially from continental basaltic magmas [29], associated with a stage of continental breakup [26]. Furthermore, the amount of some trace elements including Ba (771 mg/kg), Th (0.33 mg/kg), La (4.80 mg/kg) and Nb (2.20 mg/kg) is lower than that observed in gabbro derived from the enriched mantle and higher than the average values of the primitive mantle, but consistent with the average values of the middle crust except for Ba (Ba: 400–700 mg/kg, Th: 6–8 mg/kg, La: 17–36 mg/kg, and Nb: 6–11 mg/kg) [28].

Table 2. Mass balance evaluation of major elements, trace elements and REE (%) for the soil profile samples in the Maroua region (Cameroon).

	Ma2	Ma3	Ma4	Ma5	Ma6	Mean Mobilization Rate
ε-Th	31.36	95.07	116.71	98.96	−20.18	/
SiO_2	13.33	62.88	46.50	−5.89	−68.55	9.65
Al_2O_3	−5.80	30.09	26.14	−14.49	−71.60	−7.13
Fe_2O_3	8.46	54.98	45.97	−0.24	−65.99	8.64
CaO	−88.63	−33.72	−53.49	−71.79	−83.77	−66.28
MgO	−68.08	−61.57	−64.37	−78.19	−92.24	−72.89
Na_2O	75.00	159.8	162.00	26.64	−63.42	72.00
K_2O	−58.15	−65.38	−64.00	−81.70	−92.24	−72.29
TiO_2	−1.88	49.00	44.00	−5.00	−68.41	3.54
MnO	37.75	103.00	94.11	63.00	−52.00	49.17
P_2O_5	17.09	110.00	44.37	−64.32	−85.00	4.43
Ba	−45.00	−42.00	−30.00	−57.00	−87.35	−52.27
Cr	−83.00	−76.00	−82.26	−86.00	−91.21	−83.69
Cs	−60.08	31.25	3.12	−33.11	−54.58	−22.68
Ga	22.15	62.30	50.27	8.20	−62.00	16.18
Hf	31.79	57.14	45.00	−7.00	−57.00	13.99
Nb	25.80	50.00	44.00	1.35	−59.00	12.43
Rb	−72.20	−73.13	−75.37	−85.36	−91.00	−79.41
Sn	6.45	50.00	38.00	−10.81	−70.00	2.73
Sr	−5.00	57.00	3.01	−32.26	−67.02	−8.85
Ta	112.89	50.00	38.00	78.38	−39.45	47.96
Th	0.00	0.00	0.00	0.00	0.00	0.00
U	−8.00	−0.00	0.83	−17.00	−29.35	−10.70
V	−1.20	40.00	14.00	−14.48	−68.06	−5.95
Y	38.24	87.00	72.34	−8.96	−60.00	25.72
Zr	36.19	61.03	42.00	−0.32	−53.25	17.13
Co	−34.50	−0.00	−15.38	−31.39	−80.00	−32.25
Cu	−92.00	−95.31	−98.00	−86.06	−86.00	−91.47
Ni	−87.00	−81.44	−83.00	−90.00	−96.25	−87.54
Sc	18.00	77.00	67.00	15.00	−63.23	22.75
Zn	114.21	187.04	163.11	75.07	−51.03	97.68
La	53.02	91.00	104.00	35.64	−37.55	49.22
Ce	46.05	76.00	67.34	28.00	−45.31	34.42
Pr	39.49	77.47	86.00	21.00	−50.00	34.79
Nd	39.78	83.33	94.44	21.62	−52.00	37.43

Table 2. *Cont.*

	Ma2	Ma3	Ma4	Ma5	Ma6	Mean Mobilization Rate
Sm	40.76	89.48	90.00	18.00	−54.00	36.85
Eu	49.58	116.00	115.00	37.00	−47.00	54.12
Gd	37.66	86.00	87.47	16.01	−58.42	33.74
Tb	38.22	83.58	83.00	10.49	−60.23	31.01
Dy	−42.36	81.46	76.00	8.11	−61.38	12.37
Ho	38.00	79.00	77.00	8.44	−61.00	28.29
Er	35.00	80.00	64.45	4.17	−62.46	24.23
Tm	39.00	79.17	68.05	7.00	−62.15	26.21
Yb	43.05	83.26	67.00	7.00	−61.00	27.86
Lu	42.00	75.00	49.00	2.00	−60.47	21.51

4.2. Petrology of Weathered Materials

The studied soils are characterised by very low thickness (~2 m), largely dominated by that of the saprolite (≈1.70 m) at the base of the profile. This low thickness might be due to the dry Sahelian climate, which did not allow for intense chemical weathering. The main secondary minerals are montmorilonite, kaolinite and goethite, largely dominated by montmorillonite in all horizons, associated with a small amount of sepiolite, brucite, gibbsite, lepidocrocite, calcite, quartz and feldspar. This mineral assemblage is characteristic of semi-arid areas [23,30,31]. The development of montmorillonite, calcite and fibrous clay as sepiolite is characteristic of a confined and consequently less acidic environment, confirmed by the high pH obtained [31]. This mineral assemblage, in addition to a slight to moderate accumulation of Si, Fe, Na, Ti, Mn and P, and a slight to moderate depletion of Al, Ca, Mg and K, is characteristic of a conservatory geochemical mineral assemblage [32]. During the dry and warm season, soil solutions enriched in siliceous and alkaline earth rise up towards the surface; organic matter, being almost rapidly mineralized under this climate, intervenes very little. These conditions are then favourable to the formation and preservation of 2:1 clay of a montmorillonite type, characteristic of a predominance of the bisiallitisation process [23]. The presence of kaolinite and gibbsite results in monosiallitisation and allitisation processes, which, although weak, are characteristic of tropical regions [33].

4.3. Behaviour of Trace Elements

Among the trace elements detected, Ba, Cr, Sr, V, Zr and Zn concentrations are high. Except for Zr and Zn, all those elements were depleted, accompanied in this process by Rb, Co, Cu, Ni, Cs and U. However, concentrations of Ga, Hf, Nb, Ta, Y, Zr, Pb, Sc and Zn increase from the bedrock to coarse saprolite. This might have been caused by their passive accumulation, as other rock constituents that were transported into percolating groundwater were probably enhanced by the high oxygen fugacity of the soil in the lowly saturated zone nearest to the atmosphere [2]. The slight increase of Cr, Cs, Sr, Th, U, V, Zr, Cu and even Pb concentrations in the upper humiferous surface horizon might be due to intense biological activity and recycling process by certain plants [34,35]. Ba, Cr, Rb, V, Co, Cu, Li and Ni concentrations decrease from the bedrock to the coarse saprolite. This might be related to the chemical weathering, which gives rise to the destruction of their primary host minerals [36], and certainly the absence of secondary host minerals for these elements under a Sudano-Sahelian climate.

4.4. Behaviour of REE

The weathering of the parent rocks causes a mobilization of elements and fractionation of REE [37,38]. Thus, REE are released from primary minerals and absorbed by or adsorbed onto all types of secondary minerals' surface coatings [38]. According to the same authors, pH is the dominant parameter controlling REE behaviour. Under acidic conditions, REE are easily removed from weathering products, but they are fixed by major scavengers under neutral to alkaline conditions [39].

The negative Ce anomaly observed in the studied soils showed that cerium exists in trivalent form as other REE [40]. The positive Eu anomalies might be due to either the dissolution of feldspars or to other supergene mechanisms [41]. Europium might partially substitute Ca^{2+} and Sr^{2+} in feldspar [42,43].

4.5. Mass Balance Evaluation

In the weathering mantle over the gabbro in the Maroua region, some elements are leached throughout the studied soil profile. These include Ca, Mg, Ba, Cr, Rb, Co, Cu, Ni, Al, Cs, Sr, U and V. Among these elements, monovalent and divalent cations cannot be incorporated into the structures of kaolinite, gibbsite or goethite without producing an imbalance [44], and montmorillonite cannot incorporate them since Na is already enriched in all parts of the profile and might be incorporated into the interlayer space of this mineral. Al is pH-dependent. Under an alkaline pH such as that of Maroua region, it is present in soils mostly as AlO^{-} or $Al(OH)^{2-}$. It can form strong complexes with soil organic matter but oxidation might induce reducing processes, leading to the mobility of Al and thus to their leaching out of the profile [3]. U, V and Cr show similar behaviour. Their depletion in the study soil, concomitantly to the accumulation of Fe, distance the soil of the Maroua region from the characteristics of lateritic weathering currently described by several authors in the intertropical zone [45,46]. This is confirmed by the high expression of 2:1 phyllosilicate of montmorillonite type.

Elements accumulated during weathering are Si, Th, Fe, Na, Ti, Mn, P, Ga, Hf, Nb, Sn, Ta, Y, Zr, Sc, Zn and REE. Among these elements, tetravalent (Si^{4+}, Ti^{4+}, Zr^{4+} and Th^{4+}) and pentavalent (Nb^{5+} and P^{5+}) cations crystallise into silicate, phosphate and oxide minerals that are very resistant to weathering and thus persist and accumulate [44]. Thorium might exist in soils as thorite ($ThSiO_4$), monazite [(Ce, La, Th, Nd)PO_4] and thorianite (ThO_2) [47]. Although these minerals are very resistant, after extreme weathering monazite and thorite end up being dissolved and Th then precipitates as thorianite (ThO_2). Thorium is probably the most immobile of all chemical elements, even less immobile than Ti [44,48]. Niobium is a substituent in very resistant minerals because it replaces Zr in zircon and Ti in rutile [44]. Hafnium, an immobile element as Ti and Zr, is mainly associated with zircon [36]. Trivalent elements (Sc, Y, Ga and Fe) probably accumulate during weathering because they can be incorporated into the octahedral sites of secondary minerals without causing any charge imbalance [44]. The accumulation of Zn^{2+} might be due to its incorporation in the iron minerals [44], sorption which is pH-dependent, weak at pH < 6 and could thus be strong in the studied soils characterised by high pH (6.5 to 7.8). The accumulation of Mn and Na can be explained by their incorporation into the structure of montmorillonite. Furthermore, Mn might also crystallise into Mn oxides. Na enrichment, on the other hand, might be related to the long dry season of eight months.

All REE are depleted in the humiferous surface horizon. This might be due to hydrolysis in the upper part of the soils, which causes their leaching and their accumulation at the bottom of the soil profile [49], a process enhanced here by organic matter. It might also be linked to the dissolution of REE bearers in this part of the studied soils [50]. Their accumulation in the studied soils and essentially under the humiferous surface horizon is the result of the alkaline conditions noted here [39,51]. Also, REE are easily adsorbed onto 2:1 clay minerals, which predominate in the studied soils, particularly the LREE [52]. The depletion of Dy at the bottom of the coarse saprolite could be linked to the fact that Dy might exist in the bedrock as carbonate ($Dy_2(CO_3)_3$) or sulphate ($Dy_2(SO_4)_3$), resulting from the combination of Dy with various non-metals at high temperature [53]. These compounds are soluble in water and could also react with the Ca present in soil under prevalent dry tropical Sahelian climate to form calcite and anhydrite [53]. This might result in the liberation of Dy in the soil solution and its subsequent depletion at the bottom of the coarse saprolite. Similar results were reported by Aubert et al. [54] and Migaszewski and Gałuszka [55].

5. Conclusions

The studied soils are developed under a Sudano-Sahelian climate on gabbro. Their thickness is very small, largely dominated by coarse saprolite. They were mainly composed of montmorillonite, sepiolite, brucite, kaolinite, gibbsite, goethite, lepidocrocite, microcline, calcite and quartz, a mineral assemblage characteristic of a confined and less acidic environment, where the bisiallitisation process predominates.

Geochemically, these soils are characterised by an accumulation of Si, Fe, Na, Ti, Mn, P and slight to moderate depletion of Al, Ca, Mg, and K, synonymous with conservatory geochemical mineral assemblage. Trace element contents are globally low. Among them, only Ba, Cr, Sr, V, Zr and Zn concentrations are high, with values higher than 150 mg/kg. $(La/Yb)_N$ shows low fractionation between LREE and HREE, ranging between 1.04 and 1.59. The normalized data with respect to the parent rock reveal slight negative Ce anomalies, mainly in the middle part of the soils, with weak to moderate Eu anomalies in all the weathering materials. Some trace elements are depleted throughout the studied soil profile. They include Ba, Cr, Rb, Co, Cu, Ni, Al, Cs, Sr, U and V. Among these elements, monovalent and divalent cations cannot be incorporated into the structures of secondary minerals without producing an imbalance. Al, U, V and Cr can form strong complexes with soil organic matter, and oxidation might induce reducing processes, leading to their mobility and thus to their leaching out of the profile. Those that were accumulated are Th, Ga, Hf, Nb, Sn, Ta, Y, Zr, Sc, Zn and REE. They crystallise into silicate and oxide minerals that are very resistant to weathering, particularly under the Sudano-Sahelian climate, and thus persist and accumulate. Trivalent elements (Sc, Y, Ga) probably accumulate during weathering because they can be incorporated into the octahedral sites of secondary minerals without causing any charge imbalance. Also, REE are easily adsorbed onto 2:1 clay minerals, which predominate in the studied soils.

Acknowledgments: The authors thank Merlin Gountié Dedzo for assistance with fieldwork and petrographic analyses. Also, special thanks go to Sylvestre Ganno for the financial support for chemical analyses and Primus Azinwi Tamfuh for proofreading the final manuscript.

Author Contributions: This work was carried out in collaboration between all authors. All authors read and approved the final manuscript.

Conflicts of Interest: The authors declare no conflict of interest.

References

1. Muller, J.-P.; Calas, G. Tracing kaolinites through their defect carters: Kaolinite paragenesis in a laterite (Cameroon). *Econ. Geol.* **1989**, *84*, 694–707. [CrossRef]
2. Ndjigui, P.-D.; Bilong, P.; Bitom, D.; Dia, A. Mobilization and redistribution of major and trace elements in two weathering profiles developed on serpentinites in the Lomié ultramafic complex, South-East Cameroon. *J. Afr. Earth Sci.* **2008**, *50*, 305–328. [CrossRef]
3. Tsozué, D.; Bitom, D.; Lucas, Y. Biogeochemistry of Iron, Aluminium and Silicon in Humid Tropical Mountainous Soils (Bambouto Mountain, West Cameroon). *Open Geol. J.* **2009**, *3*, 70–81.
4. Lambiv Dzemua, G.; Gleeson, S.A.; Schofield, P.F. Mineralogical characterization of the Nkamouna Co–Mn laterite ore, southeast Cameroon. *Int. J. Geol. Mineral. Geochem. Miner. Depos.* **2013**, *48*, 155–171. [CrossRef]
5. Muller, J.P.; Manceau, A.; Calas, G.; Allard, T.; Ildefonse, P.; Hazemann, G. Crystal chemistry of kaolinite and Fe-Mn oxides: Relation with formation conditions of low temperature systems. *Am. J. Sci.* **1995**, *295*, 1115–1155. [CrossRef]
6. Braun, J.J.; Viers, J.; Dupre, B.; Polve, M.; Ndam, J.; Muller, J.-P. Solid/liquid REE fractionation in the lateritic system of Goyoum, East Cameroon: The implication for the present dynamics of the soil covers of the humid tropical regions. *Geochim. Cosmochim. Acta* **1998**, *62*, 273–299. [CrossRef]
7. Bayiga, E.C.; Bitom, D.; Ndjigui, P.-D.; Bilong, P. Mineralogical and geochemical characterization of weathering products of amphibolites at SW Eséka (Northern border of the Nyong unit, SW Cameroon). *J. Geol. Miner. Res.* **2011**, *3*, 281–293.

8. Nguetnkam, J.P.; Villiéras, F.; Kamga, R.; Ekodeck, G.E.; Yvon, J. Mineralogy and geochemical behaviour during weathering of greenstone belt under tropical dry conditions in the extreme North Cameroon (Central Africa). *Chemie Erde-Geochem.* **2014**, *74*, 185–193. [CrossRef]
9. Suchel, J.-B. Les climats du Cameroun. Ph.D. Thesis, Université de Bordeaux III, Pessac, France, 1987; p. 1186.
10. Letouzey, R. *Notice Explicative de la Carte Phytogéographique du Cameroun à L'échelle de 1/500000*; Institut de la Carte Internationale de la Végétation: Toulouse, France, 1985; p. 240. (In French)
11. Kouske, A.P.; Suh, C.E.; Ghogomu, R.T.; Ngako, V. Na-Metasomatism and Uranium Mineralization during a Two-Stage Albitization at Kitongo, Northern Cameroon: Structural and Geochemical Evidence. *Int. J. Geosci.* **2012**, *3*, 258–279. [CrossRef]
12. Dumort, J.C.; Peronne, Y. *Notice Explicative sur la Feuille Maroua. 1 Carte géologique de Reconnaissance au1/500000*; Direction des Mines et de la Géologie: Yaoundé, Cameroon, 1966.
13. Lasserre, M. Etude de Géologique et prospection générale orientée du complexe volcano-sédimentaire Tcholliré-Bibemi-Maroua. In *Mesures géochronologiques sur les formations du Nord Cameroun par les méthodes au rubidium/strontium et au potassium/argon sur minéraux et roches totals*; Direction des Mines et de la Géologie: Yaoundé, Cameroon, 1975; p. 37. (In French)
14. Guitián, O.F.; Carballas, T. *Técnicas de análisis de Suelos [Techniques of Soil Analysis]*; Pico Sacro: Santiago de Compostela, Spain, 1976; p. 288. (In Spanish)
15. Blake, G.R.; Hartge, K.H. *Bulk Density, in Methods of Soil Analysis Part 1. Physical and Mineralogical Methods*; Agronomy Monograph No. 9; Soil Science Society of America: Madison, WI, USA, 1986; pp. 363–373.
16. USDA. *Soil Survey Laboratory Methods Manual*; Soil Survey Investigations Report 2004; United States Department of Agriculture, Natural Resources Conservation Service: Washington, DC, USA, 2004; Volume 42, p. 700.
17. Brimhall, G.H.; Dietrich, W.E. Constitutive mass balance relations between chemical composition, volume, density, porosity and strain in metasomatic hydrochemical systems: Results on weathering and pedogenesis. *Geochim. Cosmochim. Acta* **1987**, *51*, 567–587. [CrossRef]
18. Colin, F.; Brimhall, G.H.; Nahon, D.; Lewis, C.J.; Baronnet, A.; Danty, K. Equatorial rainforest lateritic mantles: A geomembrane filter. *Geology* **1992**, *20*, 523–526. [CrossRef]
19. Colin, F.; Veillard, P.; Ambrosi, J.-P. Quantitative approach to physical and chemical gold mobility in equatorial rainforest lateritic environment. *Earth Planet. Sci. Lett.* **1993**, *114*, 269–285. [CrossRef]
20. Brimhall, G.H.; Alpers, C.N.; Cunningham, A.B. Analysis of supergene ore–forming processes and grand—Water solute transport using mass balance principles. *Econ. Geol.* **1985**, *80*, 1227–1256. [CrossRef]
21. Middlemost, E.A.K. Naming materials in the magma/igneous rock system. *Earth Sci. Rev.* **1994**, *37*, 215–224. [CrossRef]
22. McDonough, W.F.; Sun, S.S. The composition of the earth. *Chem. Geol.* **1995**, *120*, 223–253. [CrossRef]
23. Nguetnkam, J.P.; Kamga, R.; Villiéras, F.; Ekodeck, G.E.; Yvon, J. Variable weathering response of granite in tropical zones. Example of two sequences studied in Cameroon (Central Africa). *C. R. Geosci.* **2008**, *340*, 451–461. [CrossRef]
24. Mella, W.; Mermut, A.R. Genesis and mineralogy of soils formed on uplifted coral reef in West Timor, Indonesia. *Geoderma* **2010**, *154*, 544–553. [CrossRef]
25. Lewis, D.G.; Farmer, V.C. Infrared absorption of surface hydroxyl groups and lattice vibrations in lepidocrocite (γ-FeOOH) and boehmite (γ-ALOOH). *Clay Miner.* **1986**, *21*, 93–100. [CrossRef]
26. Toteu, S.F.; Michard, A.; Bertrand, J.M.; Rocci, G. U–Pb dating of Precambrian rocks from northern Cameroon, orogenic evolution and chronology of the Pan-African belt of central Africa. *Precambr. Res.* **1987**, *37*, 71–87. [CrossRef]
27. Ruy, P.P.; Marcelo, L.; Lauro, V.S.N. Petrology of dioritic, tonalitic and trondhjemitic gneisses from Encantadas Complex, Santana da Boa Vista, southernmost Brazil: Paleoproterozoic continental-arc magmatism. *Anais da Academia Brasileira de Ciências* **2008**, *80*, 735–748.
28. Torkian, A.; Sepahi, A.A. Petrology and geochemistry of the dioritic and granodioritic-granitic magma, Gqorveh granitoid complex (GGC), Sanandaj-Sirjan zone, Western Iran. In Proceedings of the 1st International Applied Geological Congress, Department of Geology, Islamic Azad University, Mashad Branch, Iran, 26–28 April 2010; pp. 26–28.

29. Thompson, R.N.; Morrison, M.A.; Henory, G.L.; Parry, S.J. An assessment of the relative roles of crust and mantle in magma genesis: An elemental approach. *Philos. Trans. R. Soc. Lond. A* **1984**, *310*, 549–590. [CrossRef]
30. Haritash, A.K.; Baskar, R.; Sharma, N.; Paliwal, S. Impact of slate quarrying on soil properties in semi-arid Mahendragarh in India. *Environ. Geol.* **2006**, *51*, 1439–1445. [CrossRef]
31. Francis, M.L.; Fey, M.V.; Ellis, F.; Poch, R.M. Petroduric and 'petrosepiolitic' horizons in soils of Namaqualand, South Africa. *Span. J. Soil Sci.* **2012**, *2*, 8–25.
32. Duchaufour, P. *Pédologie. Tome 1: Pédogenèse et Classification*; Masson: Paris, France, 1977; p. 477. (In French)
33. Pedro, G. Essai sur la caractérisation géochimique des différents processus zonaux résultant de l'altération des roches superficielles (cycle alumino-silicique). *C. R. Acad. Sci.* **1966**, *262*, 1828–1831. (In French)
34. Kabata-Pendias, A. *Traces Elements in Soils and Plants*, 3rd ed.; CRC Press: Boca Raton, FL, USA, 2001; p. 413.
35. Lucas, Y. The role of plants in controlling rates and products of weathering: Importance of biological pumping. *Annu. Rev. Earth Planet. Sci.* **2001**, *29*, 135–163. [CrossRef]
36. Rao, W.; Tan, H.; Jiang, S.; Chen, J. Trace element and REE geochemistry of fine- and coarse-grained sands in the Ordos deserts and links with sediments in surrounding areas. *Chem. Erde Geochem.* **2011**, *71*, 155–170. [CrossRef]
37. Ji, H.H.; Wang, S.; Ouyang, Z.; Zhang, S.; Sun, C.; Liu, X.; Zhou, D. Geochemistry of red residua underlying dolomites in karst terrains of Yunnan-Guizhou Plateau. I. The formation of the Pingba profile. *Chem. Geol.* **2004**, *203*, 1–27. [CrossRef]
38. Karadağ, M.M.; Küpeli, Ş.; Arýk, F.; Ayhan, A.; Zedef, V.; Döyen, A. Rare earth element (REE) geochemistry and genetic implications of the Mortaş-bauxite deposit (Seydişehir/Konya-Southern Turkey). *Chem. Erde Geochem.* **2009**, *69*, 143–159. [CrossRef]
39. Fleet, A.J. Aqueous and sedimentary geochemistry of the rare earth elements. In *Rare Earth Element Geochemistry*; Hendersonm, P., Ed.; Elsevier: Amsterdam, The Netherlands, 1984; pp. 343–373.
40. Marsh, J.S. REE fractionation and Ce anomalies in weathered Karoo dolerite. *Chem. Geol.* **1990**, *90*, 189–194. [CrossRef]
41. Ndjigui, P.-D.; Badinane, M.F.B.; Nyeck, B.; Nandjip, H.P.K.; Bilong, P. Mineralogical and geochemical features of the coarse saprolite developed on orthogneiss in the SW of Yaoundé, South Cameroon. *J. Afr. Earth Sci.* **2013**, *79*, 125–142. [CrossRef]
42. Gromet, P.L.; Silver, L.T. Rare earth element distributions among minerals in a granodiorite and their petrogenetic implications. *Geochim. Cosmochim. Acta* **1983**, *47*, 925–939. [CrossRef]
43. Panahi, A.; Young, G.M.; Rainbird, R.H. Behavior of major and trace elements (including REE) during Paleoproterozoic pedogenesis and diagenetic alteration of an archaean granite near Ville Marie, Québec, Canada. *Geochim. Cosmochim. Acta* **2000**, *64*, 2199–2220. [CrossRef]
44. Marques, J.J.; Schulze, D.G.; Curi, N.; Mertzman, S.A. Trace element geochemistry in Brazilian Cerrado soils. *Geoderma* **2004**, *121*, 31–43. [CrossRef]
45. Muller, D.; Bocquier, G.; Nahon, D.; Paque, H. Analyses des différenciations minéralogiques et structurales d'un sol ferrallitique à horizons nodulaires du Congo. Cah ORSTOM. *Sér. Pédol.* **1981**, *17*, 87–109. (In French)
46. Amhrosi, J.P.; Nahon, D. Petrological and geochemical differentiation of lateritic iron crust profiles. *Chem. Geol.* **1986**, *57*, 371–393. [CrossRef]
47. Braun, J.J.; Pagel, M.; Herbillon, A.; Rosin, C. Mobilization and redistribution of REEs and thorium in a syenitic lateritic profile: A mass balance study. *Geochim. Cosmochim. Acta* **1993**, *57*, 4419–4434. [CrossRef]
48. Mathieu, D.; Bernat, M.; Nahon, D. Short-lived U and Th isotope distribution in a tropical laterite derived from granite (Pitinga river basin, Amazonia, Brazil): Application to assessment of weathering rate. *Earth Planet. Sci. Lett.* **1995**, *136*, 703–714. [CrossRef]
49. Kamgang, K.B.V.; Onana, V.L.; Ndome Effoudou Priso, E.; Parisot, J.-C.; Ekodeck, G.E. Behaviour of REE and mass balance calculations in a lateritic profile over chlorite schists in South Cameroon. *Chem. Erde Geochem.* **2009**, *69*, 61–73. [CrossRef]
50. Boulangé, B.; Colin, F. Rare earth element mobility during conversion of nepheline syenite into lateritic bauxite at Passo Quatro, Minas Gerais, Brazil. *Appl. Geochem.* **1994**, *96*, 701–711. [CrossRef]
51. Nesbitt, H.W. Mobility and fractionation of rare earth elements during weathering of a granidiorite. *Nature* **1979**, *279*, 206–210. [CrossRef]

52. Laufer, F.; Yariv, S.; Steinber, M. The adsorption of quadrivalent cerium by kaolinite. *Clay Miner.* **1984**, *19*, 137–149. [CrossRef]
53. Heiserman, D.L. *Exploring Chemical Elements and Their Compounds*; TAB Books: Blue Ridge Summit, PA, USA, 1992; pp. 236–238.
54. Aubert, D.; Stille, P.; Probst, A. REE fractionation during granite weathering and removal by waters and suspended loads: Sr and Nd isotopic evidence. *Geochim. Cosmochim. Acta* **2001**, *65*, 387–406. [CrossRef]
55. Migaszewski, Z.M.; Gałuszka, A. The Characteristics, Occurrence, and Geochemical Behavior of Rare Earth Elements in the Environment: A Review. *Crit. Rev. Environ. Sci. Technol.* **2015**, *45*, 429–471. [CrossRef]